SEZONSKA SPREMENLJIVOST ČASOVNIH VRST GPS-KOORDINAT NA PODLAGI ANOVA-VARIANC

SEASONAL PATTERN IN TIME SERIES OF VARIANCES OF GPS RESIDUAL ERRORS ANOVA ESTIMATES

Darko Anđić

UDK: 528.28
Klasifikacija prispevka po COBISS.SI: 1.01
Prispelo: 26. 2. 2019
Sprejeto: 23. 5. 2019

DOI: 10.15292/geodetski-vestnik.2019.02.260-271
SCIENTIFIC ARTICLE
Received: 26. 2. 2019
Accepted: 23. 5. 2019

IZVLEČEK

V prispevku predstavljamo spremeljivost ANOVA-varianc časovnih vrst GPS-koordinat. Za namene analize smo določili koordinate na podlagi dvojnih faznih razlik opazovanj GPS z uporabo ionosferskega vpliva proste linearne kombinacije opazovanj (L0), ob faznih nedoločenostih, določenih v množici naravnih števil. Namen raziskave je bil ugotoviti značilnosti časovno spremenljivega obnašanja ANOVA-varianc časovne vrste koordinat in izkazalo se je, da je v časovnih vrstah koordinat prisoten sezonski vpliv. V primerjavi dnevnih in mesečnih koordinat so bile za dnevno določitev koordinat zaznane večje razlike med vrednostmi ANOVA-varianc. Pri izračunih smo uporabili podatke štirilenih opazovanj GPS za bazni vektor dolžine 40 kilometrov, pri čemer so bila opazovanja izvedena v obdobju nizke in tudi povečane Sončeve aktivnosti.

ABSTRACT

In this paper, which represents a continuation of the previous author's work, an inconstancy of GPS residual error ANOVA estimates and their variances are presented. For the purpose of the analysis, fixed solutions for all of the three coordinates, e *(eastwards),* n *(northwards) and* u *(upwards), obtained by using ionosphere-free (L0) linear combination of double-difference phase observations in the processing of GPS data, were employed. The aim of the research was to consider the behaviour of variances of GPS residual error ANOVA estimates in time because there has not been any paper dealing with that issue so far. Herein, it turned out a seasonal pattern in related time series was present. In addition, it was concluded there was a difference in ANOVA estimate extreme values obtained when one considered daily data subsets compared to those obtained in the approach considering monthly data of the fixed solutions. GPS data collected at ending stations of a baseline of 40 km in length within a four-year period, involving the lowest and increased solar activity, were used in calculations.*

KLJUČNE BESEDE

kratkoročno večpotje, vpliv troposfere in ionosfere, ANOVA, določenje položaja z GPS, sezonski vpliv

KEY WORDS

''far-field'' multipath, tropospheric and ionospheric effect, ANOVA, GPS positioning, seasonal pattern

1 INTRODUCTION

In Anđić (2016), the author proved the possibility of using the two-way nested classification with random effects with no interactions in variance components estimation for residuals arising due to the influence of multipath and the joint influence of ionospheric and tropospheric refraction with simultaneous separation of the pure error variance estimate. In other words, besides those related to the random effects, reliable ANOVA estimates for short-periodic and long-periodic residual effects were obtained. The present study, however, makes one step further, since it implies a consideration of seasonal behaviour of aforementioned ANOVA estimates and their variances.

As in Anđić (2016), the GPS infrastructure used includes two MontePos GPS permanent stations, located in Podgorica and Bar. Static-mode measurements, registered at each 30 s, are also used herein, but now during the four-year period 2008–2011, which was chosen since it involves the lowest and increased solar activity in the 11-year solar cycle. Slope distance and altitude difference between the stations are, respectively, 40 km and 38 m. Receivers and antennas at both stations are of the same type. In addition, the antennas have the same orientation. For post-processing of GPS measurements, the same software with the same settings as written in Anđić (2016) was used.

Double-difference phase observation model provides cancelling out of the effects of receiver antenna phase centre offsets and variations when it is about a short- as well as a medium-distance baseline with antennas of the same type set at both its ends (Kouba, 2009; El-Hattab, 2013). Taking into account that antennas of the same type and, even, the same orientation were set at both ends of the elected baseline of 40 km in length, one states these effects can be neglected in this study. The same can be said for the ''near-field" multipath effects, because both antennas were set in the same way and provided with the radomes of the same type, and, what is more important, there were not any prospective reflectors in the ''near-field" environment of those antennas (see Figure 1 in Anđić (2016)).

Pursuant to the abovementioned, only the joint influence of ionospheric and tropospheric refraction and the ''far-field" multipath influence are supposed to be considered herein. In publications such as Satirapod and Rizos (2005), Ragheb et al. (2007), Hsieh and Wu (2008), Rost and Wanninger (2010), Lau (2012), Azarbad and Mosavi (2014), Wang et al. (2018), one can find about multipath and its impact on GPS positioning. About ionosphere and its residual effects, a reader can find in, e.g. Kedar et al. (2003), Morton et al. (2009), Petrie et al. (2011), Sterle et al. (2013), Liu et al. (2016) and Hadas et al. (2017). Some of the recent publications dealing with tropospheric refraction modelling are e.g. Musa et al. (2004), Yahya et al. (2009) and Danasabe et al. (2015).

2 METHODS

2.1 Two-way nested ANOVA in GPS precise positioning

The method involves a linear model based on the unbalanced two-way nested classification theory where random effects with no interactions are present (Searle, 1971). The model equation is written as (for details, see Anđić (2016)):

$$\Delta_{ijk} = \alpha_i + \beta_{ij} + \varepsilon_{ijk}, \text{ with } i \in \underbrace{\{1,2,\ldots,a\}}_{W_1},\ j \in \underbrace{\{1,2,\ldots,b_i\}}_{W_2},\ k \in \underbrace{\{1,2,\ldots,n_{ij}\}}_{W_3}, \tag{1}$$

with $a \geq 2$, $b_i \geq 2$, $n_{ij} \geq 2$, and the accompanying stochastic model, based on the following assumptions:

$$\begin{aligned}
&(\forall i \in W_1)(\alpha_i \sim N(0,\sigma_\alpha^2)) ;\\
&(\forall (i,j) \in W_1 \times W_2)(\beta_{ij} \sim N(0,\sigma_\beta^2)) ;\\
&(\forall (i,j,k) \in W_1 \times W_2 \times W_3)(\varepsilon_{ijk} \sim N(0,\sigma_\varepsilon^2)) ;\\
&(\forall (i,j,k) \in W_1 \times W_2 \times W_3)(\mathrm{cov}(\alpha_i,\beta_{ij}) = \mathrm{cov}(\alpha_i,\varepsilon_{ijk}) = \mathrm{cov}(\beta_{ij},\varepsilon_{ijk}) = 0) ;\\
&(\forall (i,j,k),(p,q,r) \in W_1 \times W_2 \times W_3)((i \neq p \vee j \neq q \vee k \neq r) \Rightarrow \mathrm{cov}(\varepsilon_{ijk},\varepsilon_{pqr}) = 0) ,
\end{aligned} \tag{2a}$$

and, consequently:

$$(\forall (i,j,k) \in W_1 \times W_2 \times W_3)(\Delta_{ijk} \sim N(0,\sigma_\Delta^2)), \tag{2b}$$

where the following notations were introduced:

Δ_{ijk} – *the true error of the fixed double-difference L0 solution for the relative coordinate* ***e***, ***n*** or ***u***, *for an individual epoch*;

α_i – *the joint random effect of tropospheric and ionospheric refraction* (***the nesting factor***);

β_{ij} – *the random effect of "far-field" multipath* (***factor nested within*** α_i); and

ε_{ijk} – *the purely random error* (***nested within*** β_{ij}).

In order to make a connection with the presentation below, the next notations are introduced here:

$$N_i = \sum_{j=1}^{b_i} n_{ij} = n_{i\bullet}, \quad B = \sum_{i=1}^{a} b_i = b_\bullet, \quad N = \sum_{i=1}^{a}\sum_{j=1}^{b_i} n_{ij}. \tag{3}$$

Based on (1) and (2a-b), one can write:

$$(\forall (i,j,k) \in W_1 \times W_2 \times W_3)(\mathrm{D}\{\Delta_{ijk}\} = \sigma_\Delta^2 = \sigma_\alpha^2 + \sigma_\beta^2 + \sigma_\varepsilon^2), \tag{4}$$

where σ_α^2, σ_β^2 and σ_ε^2 are **the variance components** to be estimated.

A graphical presentation of the true error statistical distribution for the coordinates ***e***, ***n*** and ***u*** is given by frequency histograms in Figure 1, Figure 2 and Figure 3 (January 2009 is chosen as an example). It is obvious that the validity of the assumptions given by (2a-b) exists.

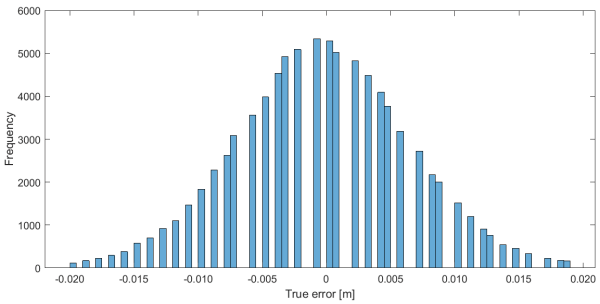

Figure 1: Frequency histogram for the true errors of the coordinate ***e*** (January 2009) – baseline Bar-Podgorica.

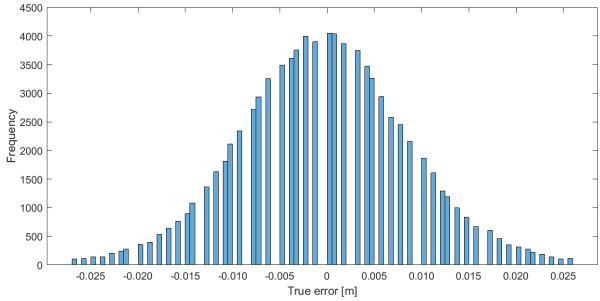

Figure 2: Frequency histogram for the true errors of the coordinate ***n*** (January 2009) – baseline Bar-Podgorica.

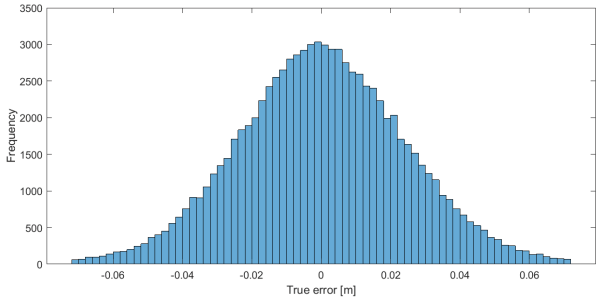

Figure 3: Frequency histogram for the true errors of the coordinate ***u*** (January 2009) – baseline Bar-Podgorica.

In this paper, separately for each coordinate, the author divided the set of all true errors for the four-year period (2008–2011) by months (not by days as in his previous research) and then, within each subset established, he carried out the same procedure as described in Anđić (2016), with exceptions of its parts regarding the step 8 (related to hypothesis testing of influence of the nesting factor α) and the step 10 (related to outlier detection method used).

As for the step 8, i.e. ***testing for statistical significance of the influence of the nesting factor*** (α), the following test statistic is used herein (following Sahai and Ojeda, 2005):

$$F_\alpha \left| H_{0,\alpha} = \frac{MSN}{MSB} \right| H_{0,\alpha} \sim F(f_{MSN}, B-a). \tag{5}$$

The sums *MSN* and *MSB*, with the corresponding degrees of freedom, are calculated as follows:

$$MSN = (\upsilon_1 / \upsilon_3)MSA + (1-\upsilon_1 / \upsilon_3)MSE, \quad f_{MSN} = \frac{MSN^2}{\frac{(\upsilon_1/\upsilon_3)^2}{a-1}MSA^2 + \frac{(1-\upsilon_1/\upsilon_3)^2}{N-B}MSE^2} \text{ d.f,} \tag{5a}$$

$$MSB = \frac{\sum_{i=1}^{a}\sum_{j=1}^{b_i} n_{ij}(n_{ij}^{-1}\sum_{k=1}^{n_{ij}}\Delta_{ijk} - N_i^{-1}\sum_{j=1}^{b_i}\sum_{k=1}^{n_{ij}}\Delta_{ijk})^2}{B-a}, \quad f_{MSB} = B-a \text{ d.f,} \tag{5b}$$

with

$$\upsilon_1 = \frac{N-k_{12}}{B-a} \quad \text{and} \quad \upsilon_3 = \frac{k_{12}-k_3}{a-1}, \tag{5c}$$

where a, B and N are from (1) and (3). Calculation of k_{12} and k_3 was given in *Anđić* (*2016*).

When $F_\alpha > F_{0.95}\,(f_{MSN}, B-a)$, there is a statistically significant influence of the nesting factor.

On the other side, as for the step 10, i.e. ***outlier detection***, beside the ''three-sigma" criterion, the PEROBHIK2S method was also used. Thus, a ''fine" elimination of gross errors was also provided. For details regarding the related mathematical tool, see *Perović* (*2015*, *2017*).

2.2 ANOVA estimates and estimates of their variances and covariances

The ANOVA estimates are calculated as follows (see also *Anđić* (*2016*)):

$$\widehat{\sigma_\varepsilon^2} = m_\varepsilon^2 = \frac{\sum_{i=1}^{a}\sum_{j=1}^{b_i}\sum_{k=1}^{n_{ij}}\Delta_{ijk}^2 - \sum_{i=1}^{a}\sum_{j=1}^{b_i} n_{ij}^{-1}\left(\sum_{k=1}^{n_{ij}}\Delta_{ijk}\right)^2}{N-B}; \tag{6}$$

$$\widehat{\sigma_\beta^2} = m_\beta^2 = \frac{\sum_{i=1}^{a}\sum_{j=1}^{b_i} n_{ij}^{-1}\left(\sum_{k=1}^{n_{ij}}\Delta_{ijk}\right)^2 - \sum_{i=1}^{a} N_i^{-1}\left(\sum_{j=1}^{b_i}\sum_{k=1}^{n_{ij}}\Delta_{ijk}\right)^2 - (B-a)m_\varepsilon^2}{N-k_{12}}; \tag{7}$$

$$\widehat{\sigma_\alpha^2} = m_\alpha^2 = \frac{\sum_{i=1}^{a} N_i^{-1}\left(\sum_{j=1}^{b_i}\sum_{k=1}^{n_{ij}}\Delta_{ijk}\right)^2 - N^{-1}\left(\sum_{i=1}^{a}\sum_{j=1}^{b_i}\sum_{k=1}^{n_{ij}}\Delta_{ijk}\right)^2 - (k_{12}-k_3)m_\beta^2 - (a-1)m_\varepsilon^2}{N-k_1}, \tag{8}$$

with **the correspondent degrees of freedom**:

$$f_\varepsilon = N - B \tag{6a}$$

$$\hat{f}_\beta = \frac{(MSB - MSE)^2}{\frac{MSB^2}{B-a} + \frac{MSE^2}{N-B}} \overset{N\to\infty}{=} f_\beta; \tag{7a}$$

$$\hat{f}_\alpha = \frac{[MSA - (\upsilon_3/\upsilon_1)MSB + (\upsilon_3/\upsilon_1 - 1)MSE]^2}{\frac{MSA^2}{a-1} + (\upsilon_3/\upsilon_1)^2\frac{MSB^2}{B-a} + (\upsilon_3/\upsilon_1 - 1)^2\frac{MSE^2}{N-B}} \overset{N\to\infty}{=} f_\alpha, \tag{8a}$$

whereby the latter two, as signified, may be regarded as theoretical ones in the case of a large number of data.

The estimates of the ANOVA estimate variances and covariances are calculated as follows (see also *Anđić* (*2016*)):

$$m_{m_\varepsilon^2}^2 = \frac{2m_\varepsilon^4}{N-B} \tag{9}$$

$$m_{m_\beta^2}^2 = \frac{2(k_7 + Nk_3 - 2k_5)m_\beta^4 + 4(N-k_{12})m_\varepsilon^2 m_\beta^2 + \frac{2(B-a)(N-a)}{N-B}m_\varepsilon^4}{(N-k_{12})^2} \tag{10}$$

$$m_{m_\alpha^2}^2 = \frac{2(\lambda_1 m_\alpha^4 + \lambda_2 m_\beta^4 + \lambda_3 m_\varepsilon^4 + 2\lambda_4 m_\alpha^2 m_\beta^2 + 2\lambda_5 m_\alpha^2 m_\varepsilon^2 + 2\lambda_6 m_\beta^2 m_\varepsilon^2)}{(N-k_1)^2(N-k_{12})^2} \tag{11}$$

$$\hat{K}_{m_\varepsilon^2, m_\alpha^2} = \frac{\frac{(k_{12}-k_3)(B-a)}{N-k_{12}} - (a-1)}{N-k_1} m_{m_\varepsilon^2}^2 \tag{12}$$

$$\hat{K}_{m_\varepsilon^2, m_\beta^2} = -\frac{B-a}{N-k_{12}} m^2_{m_\varepsilon^2} \tag{13}$$

$$\hat{K}_{m_\beta^2, m_\alpha^2} = \frac{2(k_5 - k_7 + \frac{k_6 - k_4}{N}) m_\beta^4 + \frac{2(a-1)(B-a)}{N-B} m_\varepsilon^4 - (N-k_{12})(k_{12}-k_3) m^2_{m_\beta^2}}{(N-k_1)(N-k_{12})} \tag{14}$$

and then also **the correlation coefficient estimates**:

$$\hat{r}_{m_\varepsilon^2, m_\alpha^2} = \frac{\hat{K}_{m_\varepsilon^2, m_\alpha^2}}{m_{m_\varepsilon^2} m_{m_\alpha^2}}, \quad \hat{r}_{m_\varepsilon^2, m_\beta^2} = \frac{\hat{K}_{m_\varepsilon^2, m_\beta^2}}{m_{m_\varepsilon^2} m_{m_\beta^2}} \quad \text{and} \quad \hat{r}_{m_\beta^2, m_\alpha^2} = \frac{\hat{K}_{m_\beta^2, m_\alpha^2}}{m_{m_\beta^2} m_{m_\alpha^2}}. \tag{15}$$

Remark: During the calculation process, the adopted interval-variant B from Anđić (2016) was used.

2.3 Testing homogeneity of variances within the entire four-year period considered

Bartlett's test (Bartlett, 1937) is used to test if k ANOVA estimates obtained are statistically equal. Namely, for each coordinate (***e***, ***n*** and ***u***), the test is performed particularly for nesting (α) and nested (β) factor, as well as for the pure random effect (ε). For that purpose, the following ***test statistic*** is used:

$$\chi^2_{\boldsymbol{c},i} \mid H_0 = \frac{3(k_{\boldsymbol{c},i}-1)[f_{\boldsymbol{c},i} \ln m^2_{\boldsymbol{c},i} - \sum_{p=1}^{k_{\boldsymbol{c},i}} (f_{\boldsymbol{c},i,p} \ln m^2_{\boldsymbol{c},i,p})]}{3(k_{\boldsymbol{c},i}-1) + \sum_{p=1}^{k_{\boldsymbol{c},i}} (1/f_{\boldsymbol{c},i,p}) - 1/f_{\boldsymbol{c},i}} \mid H_0 \sim \chi^2_{k_{\boldsymbol{c},i}-1} \tag{16}$$

where $(\boldsymbol{c}, i, p) \in \{\boldsymbol{e}, \boldsymbol{n}, \boldsymbol{u}\} \times \{\varepsilon, \beta, \alpha\} \times \{1, 2, \ldots, k_{\boldsymbol{c},i}\}$, and whereby the following variance with the corresponding degrees of freedom is previously calculated:

$$m^2_{\boldsymbol{c},i} = f^{-1}_{\boldsymbol{c},i} \sum_{p=1}^{k_{\boldsymbol{c},i}} f_{\boldsymbol{c},i,p} m^2_{\boldsymbol{c},i,p}, \quad \text{with} \quad f_{\boldsymbol{c},i} = \sum_{p=1}^{k_{\boldsymbol{c},i}} f_{\boldsymbol{c},i,p} \text{ d.f}, \tag{17}$$

One should note that a good approximation to χ^2– distribution is achieved when degrees of freedom are greater than or equal to 4 (Bolšev and Smirnov, 1968), and that is largely fulfilled in this study, because one states $f_{\boldsymbol{c},\alpha,p} > 74$, with $(\boldsymbol{c}, p) \in \{\boldsymbol{e}, \boldsymbol{n}, \boldsymbol{u}\} \times \{1, 2, \ldots, k_{\boldsymbol{c},\alpha}\}$ (degrees of freedom for the nesting factor, comparing to those for the nested factor and the purely random effect, always take minimal values).

So, if $\chi^2_{\boldsymbol{c},i} \leq \chi^2_{1-\alpha;k_{\boldsymbol{c},i}-1}$, then H_0 is accepted (*all variances are equal*). Otherwise, H_0 is rejected (*there is at least one variance that differs from the others*).

3 RESULTS

The results obtained by applying the procedure described in Chapter 2 are presented numerically and graphically in the continuation. At first, extreme values of square roots of ANOVA estimates, calculated by months for the coordinates ***e***, ***n*** and ***u***, are shown in Table 1. Time series graphs of those square roots are presented in Figure 4.

Maximums and minimums of the estimates of the ANOVA estimate variances are presented in Table 2, and there is also Figure 5 representing the corresponding time series.

Table 1: Maximums and minimums of the square roots of the ANOVA estimates (in mm).

	Square Roots of ANOVA Estimates	Year 2008		Year 2009		Year 2010		Year 2011	
		min	max	min	max	min	max	min	max
e	m_ε	3.3	4.6	3.7	4.6	4.1	4.5	3.8	4.5
	m_β	3.5	5.6	4.0	5.6	4.0	5.7	3.7	5.7
	m_α	2.4	4.5	2.1	5.0	2.3	5.1	2.1	5.2
n	m_ε	4.3	6.1	4.9	6.1	5.4	6.2	4.9	5.7
	m_β	4.9	7.0	5.0	6.7	5.1	7.0	4.6	6.5
	m_α	3.0	7.0	3.1	7.6	3.0	7.1	2.4	7.0
u	m_ε	8.3	13.1	8.8	12.4	10.4	12.7	9.4	10.9
	m_β	9.9	15.4	11.0	15.3	10.8	17.2	10.6	15.6
	m_α	16.6	29.7	15.6	31.1	13.5	34.5	16.4	36.5

Table 2: Maximums and minimums of the estimates of the ANOVA estimate variances (in mm^4).

	Estimates of ANOVA Estimate Variances	Year 2008		Year 2009		Year 2010		Year 2011	
		min	max	min	max	min	max	min	max
e	$m^2_{m^2_\varepsilon}$	0.0035	0.0185	0.0069	0.0150	0.0092	0.0133	0.0061	0.0369
	$m^2_{m^2_\beta}$	0.0324	0.2462	0.0626	0.1944	0.0573	0.2162	0.0428	0.2203
	$m^2_{m^2_\alpha}$	0.2038	2.8503	0.1358	3.9016	0.1978	4.3530	0.1548	4.6704
n	$m^2_{m^2_\varepsilon}$	0.0106	0.0544	0.0226	0.0481	0.0279	0.0476	0.0165	0.0950
	$m^2_{m^2_\beta}$	0.1157	0.6128	0.1348	0.4349	0.1591	0.5221	0.1157	0.3772
	$m^2_{m^2_\alpha}$	0.5399	18.6456	0.8347	21.1847	0.6035	16.4889	0.4170	16.2761
u	$m^2_{m^2_\varepsilon}$	0.1487	1.1675	0.2367	0.8474	0.4195	0.8608	0.2396	2.0631
	$m^2_{m^2_\beta}$	1.8719	14.0572	3.0859	12.0416	2.9764	16.8701	2.7603	16.4249
	$m^2_{m^2_\alpha}$	482.43	5995.81	344.02	5815.81	208.91	8562.71	460.38	11001.9

Figure 4 provides the information that a seasonal pattern in the time series of (the square roots of) the ANOVA estimates is present. It can be concluded that maximums and minimums are present in the summer and winter period, respectively. This ascertainment is also valid for the time series of the estimates of the ANOVA estimate variances (see Figure 5). The highest values exist for the coordinate ***u***. It is also obvious that values related to the coordinate ***e*** are lower than the correspondent ones, which were obtained for the coordinate ***n***.

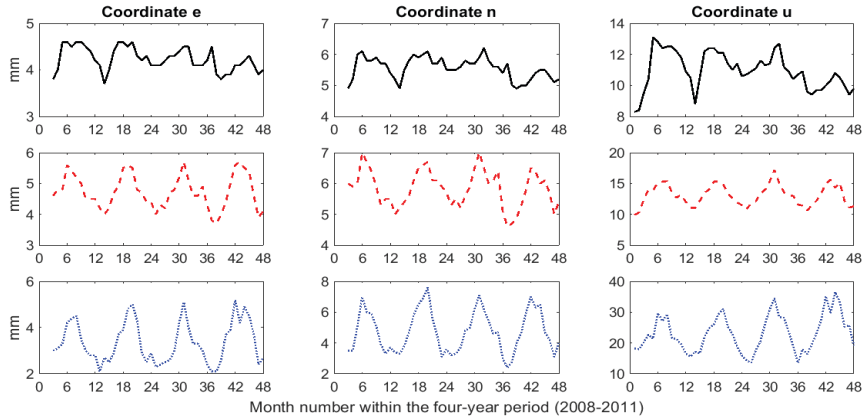

Figure 4: Time series of the square roots of the ANOVA estimates (solid – m_ε; dash – m_β; dot – m_α).

In Figure 5, one can also spot that convincingly highest values of the estimates of the ANOVA estimate variances are related to the coordinate ***u***, especially when considering the nesting factor. On the other hand, the estimates for the coordinate ***e*** are with the lowest values, no matter if the purely random effect, the nested or the nesting factor is observed, but very close to the correspondent ones for the coordinate ***n*** when considering the nested factor.

With the aim to avoid potential doubts regarding the peaks in the diagrams in the first row of Figure 5, connected to january 2011, the author want to emphasize that the correspondent values were obtained on the basis of a significantly decreased number of the true errors due to a larger percentage of rejected data in a ''fine" (i.e. additional) elimination of gross errors, by using the aforementioned PEROBHIK2S method (45.6%, 44.6% and 65.8% in the case of the coordinates ***e***, ***n*** and ***u***, respectively), which led to a decrease in denominator in equation (9), causing, in that way, an increase of the related estimate of the ANOVA estimate variance for the purely random error. The values related to the peaks weren't intentionally omitted in the diagrams to testify how a smaller input dataset affects the estimates.

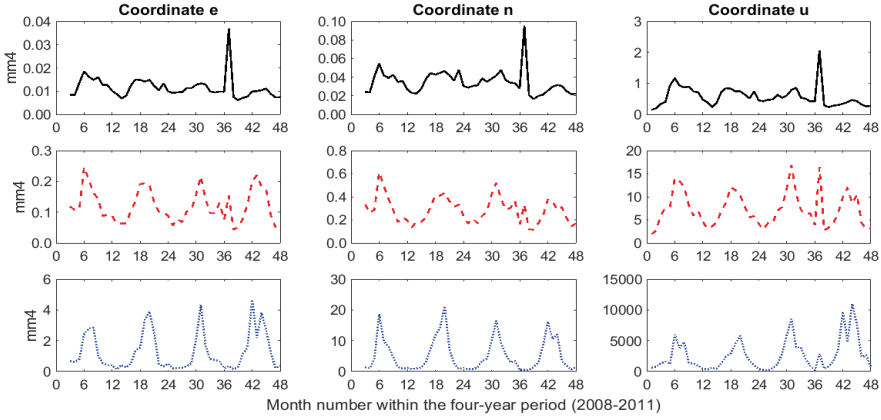

Figure 5: Time series of the estimates of the ANOVA estimate variances (solid – $\boldsymbol{m^2_{m^2_\varepsilon}}$; dash – $\boldsymbol{m^2_{m^2_\beta}}$; dot – $\boldsymbol{m^2_{m^2_\alpha}}$).

Table 3 provides an insight into the correlation of the ANOVA estimates. One can be easy concluded that there is no correlation between the ANOVA estimates for the purely random and the joint tropospheric and ionospheric effect at all, and, practically, there is no other correlation.

Table 3: Maximums and minimums of the absolute values of the ANOVA estimate correlation coefficients estimates (in %).

	Estimates of ANOVA Estimate Correlation Coefficients (Abs.Value)	Year 2008		Year 2009		Year 2010		Year 2011	
		min	max	min	max	min	max	min	max
	$\lvert \hat{r}_{m_\varepsilon^2, m_\beta^2} \rvert$	4.6	6.5	4.6	6.4	4.3	6.9	3.7	8.5
e	$\lvert \hat{r}_{m_\varepsilon^2, m_\alpha^2} \rvert$	**0.0**	**0.0**	**0.0**	**0.0**	**0.0**	**0.0**	**0.0**	**0.0**
	$\lvert \hat{r}_{m_\beta^2, m_\alpha^2} \rvert$	0.6	1.3	0.6	1.8	0.6	1.5	0.6	1.8
	$\lvert \hat{r}_{m_\varepsilon^2, m_\beta^2} \rvert$	4.6	7.6	5.6	7.2	4.9	7.4	4.5	9.3
n	$\lvert \hat{r}_{m_\varepsilon^2, m_\alpha^2} \rvert$	**0.0**	**0.0**	**0.0**	**0.0**	**0.0**	**0.0**	**0.0**	**0.0**
	$\lvert \hat{r}_{m_\beta^2, m_\alpha^2} \rvert$	0.5	1.3	0.4	1.7	0.5	1.4	0.4	2.1
	$\lvert \hat{r}_{m_\varepsilon^2, m_\beta^2} \rvert$	4.0	6.1	4.4	6.1	3.7	6.5	3.1	6.2
u	$\lvert \hat{r}_{m_\varepsilon^2, m_\alpha^2} \rvert$	**0.0**	**0.0**	**0.0**	**0.0**	**0.0**	**0.0**	**0.0**	**0.0**
	$\lvert \hat{r}_{m_\beta^2, m_\alpha^2} \rvert$	0.1	0.3	0.1	0.3	0.1	0.4	0.1	0.2

The Bartlett's test was applied within the entire four-year period (2008-2011), primarily for testing all ANOVA estimates (Approach 1), then ANOVA estimates obtained for the same months in different years (January 2008–2011, ... , December 2008–2011) (Approach 2), and, after that, for testing the ANOVA estimates obtained for the winter (January–February–March 2008–2011), spring (months: April–May–June 2008–2011), summer (months: July–August–September 2008–2011) and autumn (months: October–November–December 2008-2011) period separately (Approach 3). The significance level of 0.05 was previously adopted for all approaches, and as a homogeneity indicator, Test Statistic-to -Quantile Ratio, $\chi^2 / \chi^2_{1-\alpha;k-1}$, was chosen.

It turned out that for any effect (related to ε, β and α) and for any coordinate (***n***, ***e*** and ***u***), there is no equality in Approach 1, and the results for Approach 2 and Approach 3 are presented in Table 4.

Table 4: Summarized results of Bartlett's test applied in Approach 2 and Approach 3.

	Test Statistic-to-Quantile Ratio (Extreme and Mean Values)	Approach 2			Approach 3		
		ε	β	α	ε	β	α
e	$\min(\chi^2 / \chi^2_{0.95;k-1})$	33.67	2.75	0.75	102.75	35.94	3.10
	$\max(\chi^2 / \chi^2_{0.95;k-1})$	688.86	58.93	5.04	387.90	62.21	11.66
	$(\chi^2 / \chi^2_{0.95;k-1})_{mean}$	166.01	20.26	2.65	220.20	49.54	6.58
	Homogeneity	*no*	*no*	*for january*	*no*	*no*	*no*
n	$\min(\chi^2 / \chi^2_{0.95;k-1})$	20.59	3.24	0.52	112.85	31.13	4.65
	$\max(\chi^2 / \chi^2_{0.95;k-1})$	629.15	68.24	9.31	438.64	62.39	12.41
	$(\chi^2 / \chi^2_{0.95;k-1})_{mean}$	193.72	22.04	2.52	253.87	48.37	7.74
	Homogeneity	*no*	*no*	*for march and june*	no	no	*no*
u	$\min(\chi^2 / \chi^2_{0.95;k-1})$	104.33	1.20	0.56	350.59	35.26	4.61
	$\max(\chi^2 / \chi^2_{0.95;k-1})$	751.91	45.39	7.75	750.22	52.09	13.04
	$(\chi^2 / \chi^2_{0.95;k-1})_{mean}$	406.93	15.79	3.46	529.15	47.19	8.58
	Homogeneity	*no*	*no*	*for april*	no	no	no

The values in Table 4 show that the inhomogeneity of the residual error variances is also present between the same months from different years (with an irrelevant exception of only one or two months, listed in Table 4 for the nesting factor, Approach 2), as well as within each of the four seasons.

The results of testing in Approach 1 and Approach 2 were somewise expected, but it is not the case when it comes to the results obtained applying Approach 3.

4 DISCUSSION

On the basis of the results obtained through the study, it is obvious that the highest values of the ANOVA estimates of the ''far-field" multipath and the combined tropospheric and ionospheric residuals are present in the summer period and the lowest ones in the winter period, regardless of whether a calendar year with minimal or increased solar activity is considered. Besides, the applied statistical test provided the results proving the inhomogeneity of the residual error variances.

It turned out that the seasonal pattern in the time series of the estimates of the ANOVA estimate variances is also present, indicating extreme values that exist in the summer and winter period. In addition, there is no correlation between the ANOVA estimates for the purely random and the combined tropospheric and ionospheric effect at all, and, practically, there is no other correlation. This is stated because the absolute values of the related correlation coefficients do not exceed 9.3%.

For a GPS baseline of 40 km in length, located in the mid-latitude region, and four-year period, involving minimal and an increased solar activity, it turned out that, for the coordinates ***e***, ***n*** and ***u***, the square roots of the ANOVA estimates for the residuals arising due to the combined tropospheric and ionospheric effects are within intervals 2.1–5.2 mm, 2.4–7.6 mm and 13.5–36.5 mm, respectively. Following the same order in presenting values, for the ''far-field" residuals we have intervals 3.5–5.7 mm, 4.6–7.0 mm and 9.9–17.2 mm.

In addition, one should be noted that the part of these results obtained for the joint influence of tropospheric and ionospheric residuals during the year 2008 (see corresponding values in Table 1), in the case of the coordinates ***e*** and ***n***, is in a good agreement with the results from the first stage od the research project presented (see comments in the paragraph below Table 5 in Anđić (2016)), where those were obtained by unifying ANOVA estimates, calculated using daily subsets of data, and where intervals 1.8–3.9 mm (for the coordinate ***e***) and 2.2–6.5 mm (for the coordinate ***n***) were established. As one can see, practically, there is no significant difference between the results of the ANOVA approach based on the daily and that based on the monthly level when it is about coordinates in the horizontal plane. However, this is not the case with, always critical, coordinate ***u***. Herein we have interval 16.6-29.7 mm, which is not in so good agreement with that established in the previous research, and it is 9.4-20.2 mm. That's what was actually expected because, even if we consider a year with the lowest solar activity, there are different atmospheric conditions between different days within such a year and this had a significant impact on unifying ANOVA estimates, since a large percentage, i. e. 35% of those, was rejected through Bartlett's test (see comments above Table 5 in Anđić (2016)).

As for the multipath residual effect, comparing the results for the year 2008 presented in this paper with those given in the previous author's research, one can be said a large discrepancy exists, especially when it is about the square roots of the ANOVA estimate maximums. Namely, it turned out that the maximums ware increased 67.9%, 70.0% and 93.5% for the coordinates ***e***, ***n*** and ***u***, respectively, and, following the same order of presentation, the minimums were decreased 11.4%, 14.3% and 17.2% (to get these values, compare the related values in Table 1 to the corresponding ones for the Variant B in Table 1, Table 2 and Table 3 presented in Anđić (2016)). So, in this case, we can conclude that there is a difference between the results obtained in considering daily and monthly data subsets.

Finally, conditionally speaking, a limitation of the research presented herein exists because one cannot dispart the ionospheric and tropospheric residual effects using the methodology presented, but the implications are not limiting for practical applications since the connected results bring the joint information about the residual atmospheric effects on the precise GPS positioning.

Further research could be based on the consideration of the joint influence of tropospheric and ionospheric residuals in the daytime and nighttime particularly, using the methods presented herein. The same should be also done for the multipath residual, because of a different characteristics of prospective reflectors in these two sub-daily periods.

References:

Anđić, D. (2016). Variance Components Estimation of Residual Errors in GPS Precise Positioning. Geodetski vestnik, 60 (3), 467–482. DOI: https://doi.org/10.15292/geodetski-vestnik.2016.03.467-482

Azarbad, M. R., Mosavi, M. R. (2014). A New Method to Mitigate Multipath Error in Single-Frequency GPS Receiver with Wavelet Transform. GPS Solutions, 18 (2), 189–198. DOI: https://doi.org/10.1007/s10291-013-0320-1

Bartlett, M. S. (1937). Properties of Sufficiency and Statistical Tests. Proceedings of the Royal Society of London (pp. 268–282). Series A 160.

Bolšev, L. N., Smirnov, N. V. (1968). Mathematical Statistics (in Russion: Tablici matematičeskoj statistiki). Moscow: Vičislitelnij centr AN.

Danasabe, D. J., Mustapha, O. L., Yabayanze, T. S. (2015). Determination of the Best-Fit Tropospheric Delay Model on the Nigerian Permanent GNSS Network. Journal of Geosciences and Geomatics, 3 (4), 88–95.

El-Hattab, A. I. (2013). Influence of GPS Antenna Phase Center Variation on Precise Positioning. NRIAG Journal of Astronomy and Geophysics, 2 (2), 272–277. DOI: https://doi.org/10.1016/j.nrjag.2013.11.002

Hadas, T., Hernández-Pajares, M., Krypiak-Gregorczyk, A., Kaplon, J., Paziewski, J., Wielgosz, P., Garcia-Rigo, A., Kazmierski, K., Sosnica, K., Kwasniak, D., Sierny, J.,

Bosy, J., Pucilowski, M., Szyszko, R., Portasiak, K., Olivares-Pulido, G., Gulyaeva, T., Orus-Perez, R. (2017). Impact and Implementation of Higher-Order Ionospheric Effects on Precise GNSS Applications. Journal of Geophysical Research, 122 (11), 9420–9436. DOI: https://doi.org/10.1002/2017jb014750

Hsieh, C.-H., Wu, J. (2008). Multipath Reduction on Repetition in Time Series from the Permanent GPS Phase Residuals. The International Archives of the Photogrammetry, Remote Sensing and Spatial Information Sciences, XXXVII, Part B4, Beijing, China.

Kedar, S., Hajj, G. A., Wilson, B. D., Heflin, M. B. (2003). The Effect of the Second Order GPS Ionospheric Correction on Receiver Positions. Geophysical Research Letters, 30 (16), 1829. DOI: https://doi.org/10.1029/2003gl017639

Kouba, J. (2009). A guide to using International GNSS Service (IGS) products. http://igscb.jpl.nasa.gov/igscb/resource/pubs/UsingIGSProductsVer21.pdf, accessed on 5. 11. 2010.

Lau, L. (2012). Comparison of Measurement and Position Domain Multipath Filtering Techniques with the Repeatable GPS Orbits for Static Antennas. Survey Review, 44 (324), 9–16. DOI: https://doi.org/10.1179/1752270611y.0000000003

Liu, Z., Li, Y., Guo, J., Li, F. (2016). Influence of Higher-Order Ionospheric Delay Correction on GPS Precise Orbit Determination and Precise Positioning. Geodesy and Geodynamics, 7 (5), 369–376. DOI: https://doi.org/10.1016/j.geog.2016.06.005

Morton, Y. T., van Graas, F., Zhou, Q., Herdtner, J. (2009). Assessment of the Higher Order Ionosphere Error on Position Solutions. Navigation, 56 (3), 185–193. DOI: https://doi.org/10.1002/j.2161-4296.2009.tb01754.x

Musa, T.A., Wang, J., Rizos, C. and Lee, Y.-J. (2004). Mitigating Residual Tropospheric Delay to Improve User's Network-Based Positioning. Presented at GNSS 2004 (The 2004 International Symposium on GNSS/GPS), December 6-8, Sydney, Australia.

Perović, G. (2015). Theory of Measurement Errors (in Serbian: Teorija grešaka merenja). Belgrade: AGM knjiga.

Perović, G. (2017). Precise Geodetic Measurements (2nd extended edition) (in Serbian: Precizna geodetska merenja (drugo dopunjeno izdanje)). Belgrade: AGM knjiga.

Petrie, E. J., Hernández-Pajares, M., Spalla, P., Moore, P., King, M.A. (2011). A Review of Higher Order Ionospheric Refraction Effects on Dual Frequency GPS. Surveys in Geophysics, 32 (3), 197–253. DOI: https://doi.org/10.1007/s10712-010-9105-z

Ragheb, A. E., Clarke, P. J., Edwards, S. J. (2007). GPS Sidereal Filtering: Coordinate- and Carrier-Phase-Level Strategies. Journal of Geodesy, 81 (5), 325–335. DOI: https://doi.org/10.1007/s00190-006-0113-1

Rost, C., Wanninger, L. (2010). Carrier Phase Multipath Corrections Based on GNSS Signal Quality Measurements to Improve CORS Observations. Proceedings of IEEE/ION PLANS 2010, May 3-6, Indian Wells/Palm Springs, CA, USA.

Sahai, H., Ojeda, M. M. (2005). Analysis of Variance for Random Models, Volume II: Unbalanced Data – Theory, Methods, Applications, and Data Analysis. Boston: Birkhäuser.

Satirapod, C., Rizos, C. (2005). Multipath Mitigation by Wavelet Analysis for GPS Base Station Applications. Survey Review, 38 (295), 2–10. DOI: https://doi.org/10.1179/sre.2005.38.295.2

Searle, S. (1971). Linear Models. New York-Chichester-Weinheim-Brisbane-Singapore-Toronto: John Wiley & Sons, Inc.

Sterle, O., Stopar, B., Pavlovčič Prešeren, P. (2013). Modeliranje ionosferske refrakcije za izboljšavo absolutnega GNSS-položaja s kodnimi instrumenti: Priprava na 24. Sončev cikel (= Ionosperic refraction modeling for better autonomous GNSS code positioning: in preparation of solar cycle 24). Geodetski vestnik, 57 (1), 9–24. DOI: https://doi.org/10.15292/geodetski-vestnik.2013.01.009-024.

Wang, M., Wang, J., Dong, D., Li, H., Han, L., Chen, W. (2018). Comparison of Three Methods for Estimating GPS Multipath Repeat Time. Remote Sensing, 10 (2), 6. DOI: https://doi.org/10.3390/rs10020006

Yahya, M. H., Nordin, Z., Kamarudin, M. N. (2009). The Influence of Malaysian Troposphere on the Performance of Satellite-Based Positioning System. National Postgraduate Conference on Engineering, Science and Technology (NPC 2009), March 25-26, Universiti Teknologi PETRONAS (UTP) Campus, Bandar Seri Iskandar, Tronoh 31750, Ipoh, Perak, Malaysia.

Anđić D. (2019). Seasonal pattern in time series of variances of GPS residual errors ANOVA estimates. Geodetski vestnik, 63 (2), 260-271. DOI: https://doi.org/10.15292/geodetski-vestnik.2019.02.260-271

Darko Anđić, M.Sc.
Real Estate Administration of Montenegro
Ul. Bracana Bracanovića b.b, Podgorica, Montenegro
e-mail: andjic.darko@gmail.com